J. Korean Soc. Ind. Appl. Math. Vol.24, No.2, 143–159, 2020 http://doi.org/10.12941/jksiam.2020.24.143

A CONSISTENT DISCONTINUOUS BUBBLE SCHEME FOR ELLIPTIC PROBLEMS WITH INTERFACE JUMPS

IN KWON [1] AND GWANGHYUN JO [2]†

[1]SAMSUNG ELECTRONICS SEMICONDUCTOR R & D CENTER, HWASEONG, 18448, REPUBLIC OF KOREA

[2]DEPARTMENT OF MATHEMATICS, KUNSAN NATIONAL UNIVERSITY, GUNSAN, 54150, REPUBLIC OF KOREA

Email address: †gwanghyun@kunsan.ac.kr

ABSTRACT. We propose a consistent numerical method for elliptic interface problems with nonhomogeneous jumps. We modify the discontinuous bubble immersed finite element method (DB-IFEM) introduced in (Chang et al. 2011), by adding a consistency term to the bilinear form. We prove optimal error estimates in L^2 and energy like norm for this new scheme. One of the important technique in this proof is the Bramble-Hilbert type of interpolation error estimate for discontinuous functions. We believe this is a first time to deal with interpolation error estimate for discontinuous functions. Numerical examples with various interfaces are provided. We observe optimal convergence rates for all the examples, while the performance of early DB-IFEM deteriorates for some examples. Thus, the modification of the bilinear form is meaningful to enhance the performance.

1. INTRODUCTION

There are plenty of physical phenomena with interfaces in various disciplines including mechanical, electrical, material and petroleum engineering, etc [1, 2, 3, 4, 5, 6, 7]. Obtaining solutions (say displacement, pressure, velocity, heat flux etc) of the model equations arising from them is an important issue in relevant industry fields. However, there are some difficulties in solving them, even numerically.

Firstly, because of the abrupt change of underlying material properties, the governing equations of those problems usually have discontinuous coefficients along the interface. To handle the discontinuity, one usually uses finite element methods (FEM) or finite volume methods with fitted grids.

Received by the editors March 24 2020; Revised May 17 2020; Accepted in revised form May 27 2020; Published online June 25 2020.

2000 *Mathematics Subject Classification.* 65N12, 65N30.

Key words and phrases. Discontinuous bubble scheme, immersed finite element method, elliptic equation with interface, nonhomogeneous-jump condition, structured grids.

† Corresponding author.

Secondly, a difficulty arises when the problem has nonhomogeneous jumps across the interface. For example, thermal conduction problems in heterogeneous media may have nonhomogeneous interface conditions [6]. The potential field across the membrane of cells may be discontinuous [8]. In [9], the authors introduced some interfaces problems in dielectrophoresis where the electric flux densities and potentials have nonhomogeneous jumps along the material interface. Also, pressure and saturation variables of multiphase flows in porous media may become discontinuous when capillary pressures are discontinuous along the porous media [10, 11]. To obtain accurate numerical solutions of these problems, the jump conditions along the interface have to be handled properly. Among many numerical methods, Discontinuous Galerkin (DG) [12, 13, 14] can give accurate approximations of the nonhomogeneous jump problems, since the exact amount of jumps can be included explicitly in bilinear forms in terms of penalties. See [15], for example, for the DG schemes developed for discontinuous capillary pressures problems arising from heterogeneous porous media.

So far, most of the numerical approaches for interface problems were based on fitted grids. However, fitted grids leads to an unstructured grid, which yields a discretized system with complex data structure. Recently, new types of structured grids based methods have been developed for the interface problems in the FEM community. The first type is the extended finite element method (XFEM) [16, 17, 18, 19, 20], where one enriches the spaces by adding the truncated basis functions along the interfaces. Therefore, the number of the degrees of freedom increases on elements cut by interface.

Another structured grids based methods were introduced by by Z. Li, T. Lin and Y. Lin and their coworkers [21, 22]. Immersed finite element methods (IFEM) modifies the basis functions along the interface so that they satisfy the flux continuity conditions. The advantage of IFEM is, it does not require extra degrees of freedom like XFEM, still retains the same uniform data structures as smooth problems. The optimal error analyses of IFEM for elliptic interface probelms were given in [23, 24, 25] for the homogeneous jump cases. IFEM has been developed and applied successfully to other problems such as elasticity problem [26, 27, 28], multiphase flows in porous media [29] and Robin type elliptic problems [30]. Also, IFEM based on Crouzeix-Raviart (CR) P_1-nonconforming space [31] was developed in [24]. The advantage of P_1-nonconforming based IFEM in [24] is that the efficient computation of Darcy velocity is possible via the framework of mixed finite volume method [32].

When the problem has nonzero jumps across the interface, the discontinuous bubble IFEM (DB-IFEM) [33] was developed. In DB-IFEM [33], a discrete bubble function satisfying the given jump conditions was constructed and removed from the equation. Once the bubble function is removed, one can obtain a new problem with homogeneous jump conditions. In this way, the problem reduces to a homogeneous case with a modified right hand side, which can be solved by techniques developed earlier [33, 24]. One of the other advantages of DB-IFEM is that, it has smaller number of degrees of freedom (dof) than DG, resulting in smaller system to solve.

In this work, we modify the previous version of DB-IFEM [33]. The early version of IFEMs [21, 23, 24] for the interface problems with homogeneous jump conditions used naive bilinear form, which seemed to yield optimal results. However, it was found out that there are examples where this scheme is not optimal [34]. The scheme was improved in [35, 25] by adding the consistency terms to the bilinear form. We modify DB-IFEM given in [33] by using a similar idea. In fact, the technique of handling of consistency term has been originated from the DG community [12, 13, 14]. We provide a rigorous error analysis for L^2 and H^1-norms by proving the Bramble-Hilbert type of interpolation error estimate for discontinuous functions. We perform the numerical experiments for the proposed schemes with various interface shapes and jump conditions. We also compare the results with the early version of DB-IFEM. For all the examples we tested, we observe the optimal convergence rates in both the L^2 and H^1-norm for the new version, while the convergence rates of early version deteriorates for some examples.

The rest of the paper is organized as follows. The governing equations of elliptic problems having interface jumps and an idea of removing the jump parts with small support are described in Section 2. In Section 3, we propose a new version of DB-IFEM and the error analysis is given in Section 4. Numerical results are given in Section 5. The conclusion follows in Section 6.

2. Preliminaries

2.1. **mathematical formulation.** Let Ω be a convex domain in $\mathbb{R}^2$ which is divided by a C^2 interface Γ yielding Ω^+ and Ω^-. We consider the following second-order elliptic interface problem,

$$\begin{aligned} -\nabla \cdot \beta \nabla u &= f, \quad \text{in } \Omega \setminus \Gamma, && (2.1a)\\ [u]_\Gamma &= J_1, \quad \text{on } \Gamma, && (2.1b)\\ \left[\beta \frac{\partial u}{\partial \mathbf{n}_\Gamma}\right]_\Gamma &= J_2, \quad \text{on } \Gamma, && (2.1c)\\ u &= 0, \quad \text{on } \partial\Omega, && (2.1d) \end{aligned}$$

where $f \in L^2(\Omega)$, $J_1 \in H^{3/2}(\Gamma)$, $J_2 \in H^{1/2}(\Gamma)$ and $\mathbf{n}_\Gamma$ is a specified unit normal vector to Γ pointing from Ω^- into Ω^+ and bracket $[\cdot]_\Gamma$ means the jump across the interface, i.e., $[u]_\Gamma = u|_{\Omega^-} - u|_{\Omega^+}$. The coefficient $\beta(x)$ belongs to $C^1(\Omega^s)$, for $s = +, -$ and is a function which is discontinuous across the interface Γ. For simplicity, we assume $\beta = \beta^s$ on Ω^s ($s = +$ or $-$) are positive piecewise constants.

We introduce some function spaces and their norms. For any bounded subdomain D, we denote $D^+ = D \cap \Omega^+$, $D^- = D \cap \Omega^-$ and define $H^m(D)$ and $H_0^1(D)$ to be the usual Sobolev spaces of order m with the norm $\|\cdot\|_{m,D}$ and the semi-norm $|\cdot|_{m,D}$. For $m = 1, 2$, the space $\widetilde{H}^m(D)$ is defined as

$$\widetilde{H}^m(D) := H^m(D^+) \cap H^m(D^-),$$

with norms (semi-norms)

$$\|u\|^2_{\widetilde{H}^m(D)} := \|u\|^2_{H^m(D^+)} + \|u\|^2_{H^m(D^-)}.$$

The subspace $\widetilde{H}_0^m(D)$ is defined for $m = 1, 2$ as

$$\widetilde{H}_0^m(D) := \{u \in \widetilde{H}^m(D) \,|\, u = 0 \text{ on } \partial D\}.$$

Since the equation we want to solve has jump conditions, we need subspaces of $\widetilde{H}^m(\Omega)$ where jump conditions are imposed. We define $\mathcal{U}^{J_1,J_2}(D)$ and $\mathcal{U}_0^{J_1,J_2}(D)$ as follows:

$$\mathcal{U}^{J_1,J_2}(D) := \{\, u \in \widetilde{H}^2(D) \,|\, [u] = J_1 \text{ and } \left[\beta \frac{\partial u}{\partial \mathbf{n}}\right]_\Gamma = J_2 \quad \text{on}\, \Gamma\} \tag{2.2}$$
$$\mathcal{U}_0^{J_1,J_2}(D) := \{\, u \in \mathcal{U}^{J_1,J_2}(D) \,|\, u|_{\partial D} = 0\}.$$

The following result is given in [36, 37].

Theorem 2.1. *Assume that* $f \in L^2(\Omega)$*. Then the problem (2.1) has a unique solution* $u \in \mathcal{U}^{J_1,J_2}(\Omega)$ *such that for some constant* $C > 0$*,*

$$\|u\|_{\widetilde{H}^2(\Omega)} \le C(\|f\|_{L^2(\Omega)} + \|J_1\|_{H^{3/2}(\Gamma)} + \|J_2\|_{H^{1/2}(\Gamma)}).$$

2.2. **weak formulation with jump conditions.** We consider the weak formulation for the problem (2.1a)-(2.1d). We multiply $v \in H_0^1(\Omega)$ on each side of (2.1a) and apply Green's theorem to obtain

$$-\int_{\partial\Omega^s} \beta^s \frac{\partial u}{\partial \mathbf{n}} v ds + \int_{\Omega^s} \beta^s \nabla u \cdot \nabla v d\mathbf{x} = \int_{\Omega^s} f v d\mathbf{x}, \quad s = + \text{ or } -,$$

where $\mathbf{n}$ is a unit outward normal vector to Ω^s. Adding, we obtain

$$\int_{\Omega^+} \beta^+ \nabla u \cdot \nabla v d\mathbf{x} + \int_{\Omega^-} \beta^- \nabla u \cdot \nabla v d\mathbf{x}$$
$$= \int_\Gamma \left[\beta \frac{\partial u}{\partial \mathbf{n}_\Gamma}\right] v ds + \int_\Omega f v d\mathbf{x}, \quad \forall v \in H_0^1(\Omega).$$

Here, we define the bilinear form $a(\cdot,\cdot)$ as follows:

$$a(u, v) := \int_{\Omega^+} \beta \nabla u \cdot \nabla v d\mathbf{x} + \int_{\Omega^-} \beta \nabla u \cdot \nabla v d\mathbf{x}, \quad \forall u, v \in \widetilde{H}^1(\Omega).$$

Finally, we can rewrite the problem (2.1) as follows: Find $u \in \mathcal{U}_0^{J_1,J_2}(\Omega)$ satisfying (2.1b) and

$$a(u, v) = < J_2, v >_\Gamma + (f, v), \forall v \in H_0^1(\Omega), \tag{2.3}$$

where $(\cdot,\cdot)$ denotes the $L^2(\Omega)$ inner product and $< \cdot,\cdot >_\Gamma$ denotes the $L^2(\Gamma)$ inner product. It can be easily shown that the weak problem (2.3) is equivalent to the original problem (2.1) (see [33]).

Since the solution of the problem (2.1) belongs to $\mathcal{U}_0^{J_1,J_2}(\Omega)$ which is not a vector space, we will subtract a function corresponding to the nonhomogeneous part. There are many choices, but we will choose a function having a small support. First, we let S_Γ be a thin region containing Γ as interior (see Fig. 1, left).

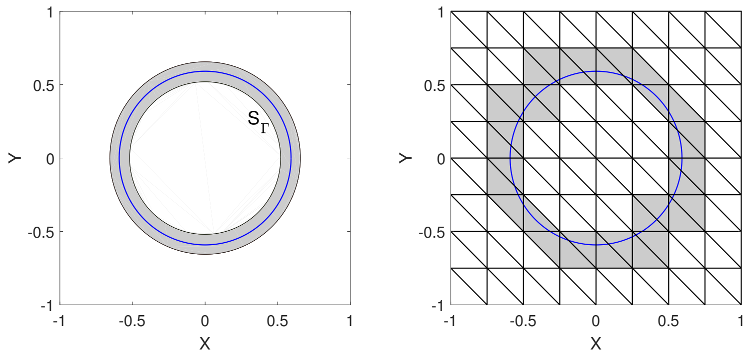

Figure 1: Example of thin strip S_Γ (left) and discretized strip S^h_Γ (right) for a given triangulation.

In practice, assuming a finite element triangulation is given, we will take S_Γ to be S^h_Γ which is the union of interface elements (see Fig. 1, right). We choose a *bubble function* u^* in $\widetilde{H}^2_0(S_\Gamma)$ which satisfies jump conditions

$$[u^*]_\Gamma = J_1,$$
$$[\beta\nabla u^* \cdot \mathbf{n}]_\Gamma = J_2.$$

Then we decompose u as follows:

$$u = u^0 + u^*,$$

where $u^0 \in H^1_0(\Omega)$.

Then we obtain a new problem:

$$\begin{aligned} -\nabla \cdot \beta\nabla u^0 &= f + \nabla \cdot \beta\nabla u^*, \quad \text{in } \Omega \setminus \Gamma,\\ [u^0]_\Gamma &= 0, \quad \text{on } \Gamma,\\ \left[\beta \frac{\partial u^0}{\partial \mathbf{n}_\Gamma}\right]_\Gamma &= 0, \quad \text{on } \Gamma,\\ u^0 &= g, \quad \text{on } \partial\Omega. \end{aligned}$$

Hence, the new variational form is following: Find $u^0 \in H^1_0(\Omega)$ satisfying

$$a(u^0, v) =< J_2, v >_\Gamma +(f, v) - a(u^*, v), \quad \forall v \in H^1_0(\Omega). \tag{2.5}$$

3. DB-IFEM

From this section on, we assume Ω is a rectangular domain. Let $\mathcal{T}_h$ be any triangulation of Ω not necessarily aligned with interface. We define $\mathcal{E}_h$ as the set of all edges of elements in $\mathcal{T}_h$. We call $T \in \mathcal{T}_h$ an interface element if T is cut by the interface Γ. Otherwise, we call T a noninterface element. We define $\mathcal{T}^*_h$ be the set of interface elements in $\mathcal{T}_h$. We define S^h_Γ to

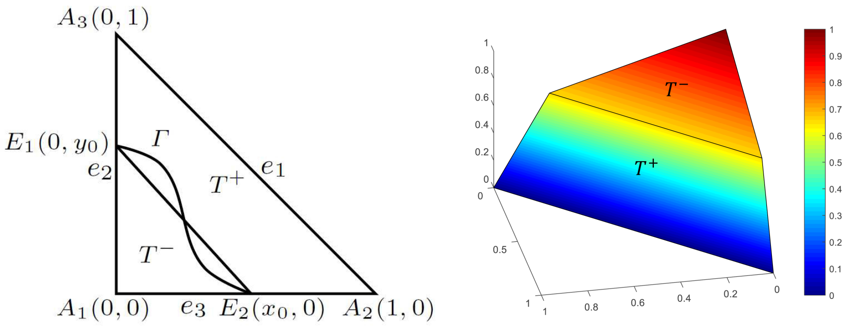

Figure 2: An interface element T (left) and the graph of $\widehat{\phi}$ on T (right).

be the union of elements in $\mathcal{T}_h^*$ (see Fig. 1). We assume that the support of u^* is S_Γ^h. In this section, we show how we discretize u^0 and u^*.

3.1. **Review of IFEM for homogeneous jumps.** First, we review the P_1-conforming based IFEM investigated in [21, 23, 24, 35, 25] for the case $J_1 = J_2 = 0$. Let T be any elements in $\mathcal{T}_h^*$. We let $S_h(T)$ be a space of standard linear functions on T with nodal dof. We show how we modify linear basis functions in $S_h(T)$. Suppose T is cut through edges e_2 and e_3 at points E_1 and E_2 respectively by Γ (see Fig. 2 (left)). Let T^+ and T^- be two regions of T separated by $\Gamma_h^T := \overline{E_1E_2}$.

Given a function $\phi \in S_h(T)$, we let $\widehat{\phi}$ be the modified piecewise linear function satisfying $\widehat{\phi}(A_i) = \phi(A_i)$ for $i = 1,2,3$ and $\left[\widehat{\phi}(E_i)\right]_{\Gamma_h^T} = 0$ for $i = 1,2$ and $\left[\beta\frac{\partial\widehat{\phi}}{\partial\mathbf{n}}\right]_{\Gamma_h^T} = 0$ (see Fig. 2 (right)). We denote the space of modified functions by $\widehat{S}_h(T)$. For noninterface element T, we do not modify. The P_1-conforming based IFEM space $\widehat{S}_h(\Omega)$ are space of all functions of $\widehat{S}_h(T)$ having vertex continuity and vanishing on boundary nodes. Given $u \in \widetilde{H}^2(T)$, we define the interpolation $I_h^0 u \in \widehat{S}_h(T)$ by

$$I_h^0 u(A_i) = u(A_i), i = 1,2,3.$$

We define $I_h^0 u$ for $u \in \widetilde{H}^2(\Omega)$ by $(I_h^0 u)|_T = I_h(u|_T)$ for each element T.

The early version of IFEM used a naive bilinear form on $H_h(\Omega) := \widehat{S}_h(\Omega) \cup \widetilde{H}_0^1(\Omega)$ defined by

$$\widetilde{a}_h(u,v) = \sum_{T\in\mathcal{T}_h} \int_T \beta\nabla u \cdot \nabla v d\mathbf{x}.$$

However, as shown later by Lin et al. [34], the result was not satisfactory for certain cases. The reason is that the consistency error is suboptimal. Hence, the bilinear form was enriched by adding the terms to handle the consistency errors [35, 25]. To handle it, we leave the line integral terms appearing from the integration by parts. We associate with a unit normal vector

$\mathbf{n}_e$ to each edge. We denote the jumps and averages for $v \in H_h(\Omega)$ across an edge $e \in \mathcal{E}_h$ by $[v]_e(x)$ and $\{v\}_e(x)$, respectively. Let

$$a_h(u,v) = \sum_{T\in\mathcal{T}_h}\int_T \beta\nabla u\cdot\nabla v\mathrm{d}\mathbf{x} - \sum_{e\in\mathcal{E}_h}\int_e \{\beta\nabla u\cdot\mathbf{n}_e\}_e[v]_e\mathrm{d}s \\ - \sum_{e\in\mathcal{E}_h}\int_e \{\beta\nabla v\cdot\mathbf{n}_e\}_e[u]_e\mathrm{d}s + \sum_{e\in\mathcal{E}_h}\frac{\sigma}{|e|}\int_e [u]_e[v]_e\mathrm{d}s, \tag{3.1}$$

where σ is a positive parameter. The optimal error estimates of IFEM with associated bilinear form in (3.1) was proven in [35, 25].

3.2. **DB-IFEM with consistentency terms.** Now we consider the case $J_1 \neq 0$ and $J_2 \neq 0$. We propose a new DB-IFEM for interface problems. We describe a *discontinuous bubble* (DB) function u_h^* introduced in [33]. Let T be element in S_Γ^h. We let u_h^* be the piecewise linear polynomial on T^+ and T^- satisfying

$$u_h^*(A_i) = 0, \quad i = 1,2,3, \tag{3.2a}$$

(3.2b)

$$[u_h^*(E_i)]_{\Gamma_h^T} = J_1(E_i), \quad i = 1,2, \tag{3.2c}$$

$$\beta^-\frac{\partial\widehat{\phi}^-}{\partial\mathbf{n}_{\Gamma_h^T}} - \beta^+\frac{\partial\widehat{\phi}^+}{\partial\mathbf{n}_{\Gamma_h^T}} = \frac{1}{|\Gamma_h^T|}\int_{\Gamma_h^T} J_2\, ds. \tag{3.2d}$$

The existence of such function is shown in [33]. Once we have determined u_h^*, we discretize weak form (2.5) using the form (3.1).

We state (consistent) DB-IFEM: Find $u_h^0 \in \widehat{S}_h(\Omega)$ such that

$$a_h(u_h^0, v) = (f,v) + \int_\Gamma J_2 v\mathrm{d}s - a_h(u_h^*, v), \tag{3.3}$$

for all $v \in \widehat{S}_h(\Omega)$. The difference between (3.3) and the form in [33] is the presence of consistent terms and stability terms in (3.1).

We show that this scheme is consistent.

Theorem 3.1. *Suppose u is a solution of (2.1a)-(2.1d) and u_h^* is the DB function defined in (3.2) and u_h^0 is the solution of (3.3). Then,*

$$a_h(u - u_h^0 - u_h^*, \phi_h) = 0 \tag{3.4}$$

for all $\phi_h \in \widehat{S}_h(\Omega)$.

Proof. In view of (3.3), it is sufficient to show that

$$a_h(u,\phi_h) = (f,\phi_h) - < J_2, \phi_h > \tag{3.5}$$

for all $\phi_h \in \widehat{S}_h(\Omega)$.

We multiply $\phi_h \in \widehat{S}_h(\Omega)$ to equation (2.1a). Applying the integration by parts on each element, and using similar techniques used in Section 2.2, we have

$$\sum_{T\in\mathcal{T}_h}\left(\int_{T\cap\Omega^-}\beta\nabla u\cdot\nabla\phi_h\,d\mathbf{x}+\int_{T\cap\Omega^+}\beta\nabla u\cdot\nabla\phi_h\,d\mathbf{x}\right)-\sum_{e\in\mathcal{E}_h}\int_e\{\beta\nabla u\cdot\mathbf{n}\}_e[\phi_h]_e ds$$
$$=(f,\phi_h)-<J_2,\phi_h>.$$

We note that $[u]_e=0$ for all $e\in\mathcal{E}_h$. Thus, by adding $-\sum_{e\in\mathcal{E}_h}\int_e\{\beta\nabla\phi_h\cdot\mathbf{n}\}_e[u]_e ds$ (to make the form symmetric) and $\frac{\sigma}{|e|}\sum_{e\in\mathcal{E}_h}[u]_e[\phi_h]_e$ to left side of the equation, we see (3.5) holds. □ □

Remark 3.1. *We can develop a similar DB scheme for the Crouzeix-Raviart IFEM* [25].

4. Error Analysis

We need the following norms on space $H_h(\Omega)$,

$$\|u\|_{1,h}:=\sum_{T\in\mathcal{T}_h}\|u\|_{\widetilde{H}^1(T)},\quad \|u\|_{E_h}:=\sum_{T\in\mathcal{T}_h}\|u\|_{E,T}.$$
$$\|u\|^2_{E,T}:=\left(\int_{T\cap\Omega^-}\beta\nabla u\cdot\nabla u\mathrm{d}x+\int_{T\cap\Omega^+}\beta\nabla u\cdot\nabla u\mathrm{d}x\right)+\sum_{e\in\partial T}\frac{1}{|e|}\int_e[u]_e^2\mathrm{d}s.$$

4.1. **Approximation property of DB.** As shown in [22], we may assume that $\Gamma\cap T$ is piecewise linear for each $T\in\mathcal{T}_h$. We define function spaces $X(T)$ and $X_\Gamma(T)$ by

$$X(T):=\widetilde{H}^2(T)$$
$$X_\Gamma(T):=\left\{u:u\in\widetilde{H}^2(T),\ \int_{\Gamma\cap T}\left[\beta\frac{\partial u}{\partial\mathbf{n}}\right]_\Gamma ds=0\right\}.$$

Note that functions in $X(T)$ or $X_\Gamma(T)$ are in general discontinuous. We also remark that $\mathcal{U}_\Gamma^{J_1,0}(T)\subset X_\Gamma(T)$ (see (2.2)).

For any $u\in X_\Gamma(T)$, we define the following norms:

$$|u|^2_{X(T)}=|u|^2_{\tilde{H}^2(T)},$$
$$\|u\|^2_{X(T)}=\|u\|^2_{\tilde{H}^1(T)}+|u|^2_{X(T)},$$
$$|\!|\!|u|\!|\!|^2_{2,T}=|u|^2_{X(T)}+\sum_{i=1}^3|u(A_i)|^2+\sum_{i=1}^2[u(B_i)]^2_\Gamma.$$

The norm $|\!|\!|\cdot|\!|\!|_{2,T}$ is similar to the one introduced in [24], where the edge dof is replaced by the vertex dof (i.e., $u(A_i)$) and jump terms $[u(B_i)]_\Gamma$ are added.

The following results can be proved in a similar fashion to the Lemma 2.4 in [24].

Lemma 4.1. $|\!|\!|\cdot|\!|\!|_{2,T}$ *is a norm in the space* $X_\Gamma(T)$ *which is equivalent to* $\|\cdot\|_{X(T)}$.

The DB function u_h^* defined in (3.2) can be viewed as an interpolation of u^* when u^* is a bubble function supported in S_Γ^h.

Lemma 4.2. *Let T be an interface element. Then for any $u \in \mathcal{U}^{J_1,J_2}(T)$, we have*

$$\|u - I_h^0 u - u_h^*\|_{m,T} \leq Ch^{2-m}\|u\|_{\tilde{H}^2(T)},\ m = 0, 1, \tag{4.1}$$

where h is the mesh size of T and u_h^* is the DB function defined in (3.2).

Proof. Let $z = u - I_h^0 u - u_h^*$. By definition,

$$\int_{\Gamma\cap T}\left[\beta\frac{\partial z}{\partial \mathbf{n}}\right]_\Gamma ds = \int_{\Gamma\cap T}\left(\left[\beta\frac{\partial u}{\partial \mathbf{n}}\right]_\Gamma - \left[\beta\frac{\partial u_h^*}{\partial \mathbf{n}}\right]_\Gamma\right) ds = J_2 - J_2 = 0.$$

Thus, $z \in X_\Gamma(T)$. Let $\widehat{T}$ be a reference interface element and let $\hat{z}(\hat{x}) := z \circ F(\hat{x})$, $\hat{u}(\hat{x}) := u \circ F(\hat{x})$ and $\widehat{u_h^*}(\hat{x}) := u_h^* \circ F(\hat{x})$ where $F : \hat{T} \to T$ is the usual affine mapping. We note the following equality holds.

$$\begin{aligned}|\!|\!|\hat{z}|\!|\!|_{2,\widehat{T}}^2 =& |\hat{z}|_{\tilde{H}^2(\widehat{T})}^2 + \sum_{i=1}^{3}|(\hat{u} - I_h^0\hat{u})(A_i)|^2 + \sum_{i=1}^{2}\left[\hat{u}(E_i) - \widehat{u_h^*}(E_i)\right]_\Gamma^2 \\ =& |\hat{u}|_{\tilde{H}^2(\widehat{T})}^2,\end{aligned} \tag{4.2}$$

since $\hat{u}(A_i) = I_h^0\hat{u}(A_i), i = 1, 2, 3$, $[\hat{u}(E_i)]_\Gamma = [\widehat{u_h^*}(E_i)]_\Gamma, i = 1, 2$, and piecewise H^2-seminorm of the piecewise linear functions $I_h^0\hat{u}$ and $\widehat{u_h^*}$ vanish. By the scaling argument for $m = 0, 1$, and the norm equivalence of $|\!|\!| \cdot |\!|\!|_{2,T}$ and $\|\cdot\|_{X(T)}$, and by (4.2) we have

$$\begin{aligned}\|u - I_h^0 u - u_h^*\|_{m,T} &\leq Ch^{1-m}\|\hat{u} - I_h^0\hat{u} - \widehat{u_h^*}\|_{m,\widehat{T}} \leq Ch^{1-m}|\!|\!|\hat{u} - I_h^0\hat{u} - \widehat{u_h^*}|\!|\!|_{2,\widehat{T}} \\ &= Ch^{1-m}|\hat{u}|_{\tilde{H}^2(\widehat{T})} \leq Ch^{2-m}|u|_{\tilde{H}^2(T)}. \quad \square\end{aligned}$$

□

Finally, we obtain the main interpolation estimate.

Theorem 4.1. *There exists a constant $C > 0$ such that*

$$\|u - I_h^0 u - u_h^*\|_{L^2(\Omega)} + h\|u - I_h^0 u - u_h^*\|_{1,h} \leq Ch^2\|u\|_{\widetilde{H}^2(\Omega)},$$

for any $u \in \mathcal{U}^{J_1,J_2}(\Omega)$.

Also, the interpolation property holds in the $\|\cdot\|_{E_h}$-norm.

Theorem 4.2. *Assume that J_1 is piecewise linear on each element. There exists a constant $C > 0$ such that*

$$\|u - I_h^0 u - u_h^*\|_{E_h} \leq Ch\|u\|_{\widetilde{H}^2(\Omega)}, \tag{4.3}$$

for any $u \in \mathcal{U}^{J_1,J_2}(\Omega)$.

Proof. We let $w = u - I_h^0 u - u_h^*$. By the assumption that J_1 is piecewise linear and by the definition of I_h^0 and u_h^*, we see that $w \in H^1(T)$ for each T.

Recalling the definition of $\|\cdot\|_{E_h}$, by Theorem 4.1 it suffices to bound $\sum_{e\in\mathcal{E}_h} \frac{1}{|e|}\int_e [w]^2 ds$. Let e be a common edge of T_1 and T_2. By the trace inequality and by (4.1)),

$$h^{-1}\int_e [w]^2 ds \le C\left(h^{-2}\|w\|^2_{L^2(T_1)} + h^{-2}\|w\|^2_{L^2(T_2)} + \|\nabla w\|^2_{L^2(T_1)} + \|\nabla w\|^2_{L^2(T_2)}\right)$$
$$\le Ch^2(\|w\|^2_{\widetilde{H}^2(T_1)} + \|w\|^2_{\widetilde{H}^2(T_2)}).$$

By summing over $e \in \mathcal{E}_h$, we reach the conclusion. □ □

4.2. **Energy and L^2-norm error estimates.** We need the following Lemma proven in [25].

Lemma 4.3. *There exists $C_0 > 0$ such that the following holds,*

$$h\|\beta\nabla\phi\cdot\mathbf{n}_e\|^2_{0,e} \le C_0\|\beta\nabla\phi\|^2_{0,T}, \tag{4.4}$$

for all $\phi \in \widehat{S}_h(T)$ and for all $T \in \mathcal{T}_h$ and $e \in \partial T$.

Now, show that $a_h(\cdot,\cdot)$ is coercive on $\widehat{S}_h(\Omega)$.

Lemma 4.4. *There exists some $C_1 > 0$ such that*

$$C_1\|\phi\|_{E_h} \le a_h(\phi,\phi),$$

holds for sufficiently large $\sigma > 0$,

Proof. Recalling the definition of $a_h(\cdot,\cdot)$, we need to bound the term $\sum_{e\in\mathcal{E}_h}\int_e\{\beta\nabla\phi\cdot\mathbf{n}\}_e[\phi]_e ds$. Suppose e is a common edge of T_1 and T_2. By Cauchy's inequality, (4.4) and Young's inequality,

$$\int_e \{\beta\nabla\phi\cdot\mathbf{n}_e\}_e[\phi]_e ds$$
$$\le h^{-1/2}\left(h^{1/2}\int_e\{\beta\nabla\phi\cdot\mathbf{n}_e\}_e^2 ds\right)^{1/2}\left(\int_e[\phi]_e^2 ds\right)^{1/2}$$
$$\le h^{-1/2}\frac{C_0}{2}\left(\|\beta\nabla\phi\|^2_{0,T_1} + \|\beta\nabla\phi\|^2_{0,T_2}\right)^{1/2}\left(\int_e[\phi]_e^2 ds\right)^{1/2}$$
$$\le \frac{\delta}{2}\left(\|\beta\nabla\phi\|^2_{0,T_1} + \|\beta\nabla\phi\|^2_{0,T_2}\right) + \frac{C_0^2}{8\delta}\left(\frac{1}{|e|}\int_e[\phi]_e^2 ds\right).$$

for any number $\delta > 0$.

$$\begin{aligned}
a_h(\phi,\phi) &= \sum_{T\in\mathcal{T}_h}\left(\int_{T^-}\beta\nabla\phi\cdot\nabla\phi d\mathbf{x} + \int_{T^+}\beta\nabla\phi\cdot\nabla\phi d\mathbf{x}\right)\\
&- 2\sum_{e\in\mathcal{E}_h}\int_e\{\beta\nabla\phi\cdot\mathbf{n}_e\}_e[\phi]_e ds + \sum_{e\in\mathcal{E}_h}\frac{\sigma}{|e|}\int_e[\phi]_e^2 ds\\
&\geq (1-3\delta)\sum_{T\in\mathcal{T}_h}\left(\int_{T^-}\beta\nabla\phi\cdot\nabla\phi d\mathbf{x} + \int_{T^+}\beta\nabla\phi\cdot\nabla\phi d\mathbf{x}\right)\\
&+ \left(\sigma - \frac{C_0^2}{4\delta}\right)\sum_{e\in\mathcal{E}_h}\frac{1}{|e|}\int_e[\phi]_e^2 ds.
\end{aligned}$$

We choose $\delta = 1/6$. If $\sigma > \frac{3C_0^2}{2}$, the desired inequality holds with

$$C_1 = \min\left\{\frac{1}{2}, \sigma - \frac{3C_0^2}{2}\right\}. \quad \square$$

□

Using similar techniques, we can easily show the boundedness of $a_h(\cdot,\cdot)$.

Lemma 4.5. *Given $\sigma > 0$, there exists some $C_2 > 0$ such that*

$$a_h(\phi,\phi) \leq C_2\|\phi\|_{E_h}.$$

for all $\phi \in \widehat{S}_h(\Omega)$.

Finally, we give the energy-norm like estimate.

Theorem 4.3. *Assume that the jump J_1 is piecewise linear. Let $u \in \mathcal{U}^{J_1,J_2}(\Omega)$ be the solution of (2.1a)-(2.1d) and $u_h^0 \in \widehat{S}_h(\Omega)$ be the solution of (3.3). If $\sigma > \frac{3C_0^2}{2}$, then the following estimates holds*

$$\|u - u_h^0 - u_h^*\|_{E_h} \leq Ch(\|f\|_{L^2(\Omega)} + \|J_1\|_{H^{3/2}(\Gamma)} + \|J_2\|_{H^{1/2}(\Gamma)}). \tag{4.5}$$

Proof. We let $w := u_h^0 - I_h^0 u \in \widehat{S}_h(\Omega)$. By the coercivity/continuity of $a_h(\cdot,\cdot)$ and by the consistency of the scheme (3.4),

$$\begin{aligned}
C_1\|w\|_{E_h}^2 &\leq a_h(w,w) = a_h(w, u_h^0 + u_h^* - u) + a_h(w, u - I_h^0 u - u_h^*)\\
&= a_h(w, u - I_h^0 u - u_h^*) \leq C_2\|w\|_{E_h}\|u - I_h^0 u - u_h^*\|_{E_h}.
\end{aligned}$$

Thus, we have

$$\|w\|_{E_h} \leq \frac{C_2}{C_1}\|u - I_h^0 u - u_h^*\|_{E_h}.$$

By the triangle inequality and by Theorem 2.1, we have the conclusion

$$\|u-u_h^0-u_h^*\|_{E_h} \le \|u-I_h^0u-u_h^*\|_{E_h}+\|w\|_{E_h}$$
$$\le \left(1+\frac{C_2}{C_1}\right)\|u-I_h^0u-u_h^*\|_{E_h} \le \left(1+\frac{C_2}{C_1}\right)C_Ih\|u\|_{\widetilde{H}^2(\Omega)}$$
$$\le Ch(\|f\|_{L^2(\Omega)}+\|J_1\|_{H^{3/2}(\Gamma)}+\|J_2\|_{H^{1/2}(\Gamma)}). \quad \square$$

□

Next, we prove the L^2-error estimate.

Theorem 4.4. *Under the same assumptions as in Theorem 4.3, we have,*

$$\|u-u_h^0-u_h^*\|_{L^2(\Omega)} \le Ch^2(\|f\|_{L^2(\Omega)}+\|J_1\|_{H^{3/2}(\Gamma)}+\|J_2\|_{H^{1/2}(\Gamma)}).$$

Proof. Let $e_h = u-u_h^0-u_h^* \in L^2(\Omega)$. Let $\psi \in H_0^1(\Omega)$ be the solution of the following problem:

$$\begin{aligned} -\nabla\cdot\beta\nabla\psi &= e_h, && \text{in } \Omega\setminus\Gamma,\\ [\psi]_\Gamma &= 0, && \text{on } \Gamma,\\ \left[\beta\frac{\partial\psi}{\partial\mathbf{n}_\Gamma}\right]_\Gamma &= 0, && \text{on } \Gamma,\\ \psi &= 0, && \text{on } \partial\Omega. \end{aligned}$$

By definition of ψ and by the integration by parts, we have

$$\|e_h\|_{L^2(\Omega)}^2 = \sum_{T\in\mathcal{T}_h}\int_T(-\nabla\cdot\beta\nabla\psi)e_h d\mathbf{x}$$
$$=\sum_{T\in\mathcal{T}_h}\left(\int_{T^-}\beta\nabla\psi\cdot\nabla e_h d\mathbf{x}+\int_{T^+}\beta\nabla\psi\cdot\nabla e_h d\mathbf{x}\right)-\sum_{e\in\mathcal{E}_h}\int_e\{\beta\nabla\psi\cdot\mathbf{n}\}[e_h]_e ds.$$

Since $\psi\in H^1(\Omega)$, we see that $[\psi]_e=0$. Thus we can add $-\sum_{e\in\mathcal{E}_h}\int_e\{\beta\nabla e_h\cdot\mathbf{n}\}_e[\psi]_e ds$ and $\sum_{e\in\mathcal{E}_h}\frac{\sigma}{|e|}\int_e[e_h]_e[\psi]_e ds$ to the right hand side, leading to the equality that

$$\|e_h\|_{L^2(\Omega)}^2 = a_h(e_h,\psi).$$

However, by the fact that $I_h^0\psi\in\widehat{S}_h(\Omega)$ and by the consistency of the scheme (3.4) we see that $a_h(e_h,\psi)=a_h(e_h,\psi-I_h^0\psi)$. Applying Cauchy's inequality and continuity of $a_h(\cdot,\cdot)$, we have

$$\|e_h\|_{L^2(\Omega)}^2 = a_h(e_h,\psi-I_h^0\psi)\le C\|e_h\|_{E_h}\cdot\|\psi-I_h^0\psi\|_{E_h}.$$

By the energy norm estimate (4.5) and by interpolation property (4.3) and by Theorem 2.1, we have

$$\|e_h\|_{L^2(\Omega)}^2 \le Ch\|u\|_{\widetilde{H}^2(\Omega)}\cdot Ch\|\psi\|_{\widetilde{H}^2(\Omega)}\le Ch\|u\|_{\widetilde{H}^2(\Omega)}\cdot Ch\|e_h\|_{L^2(\Omega)}.$$

Dividing $\|e_h\|_{L^2(\Omega)}$, we have the desired estimate. □ □

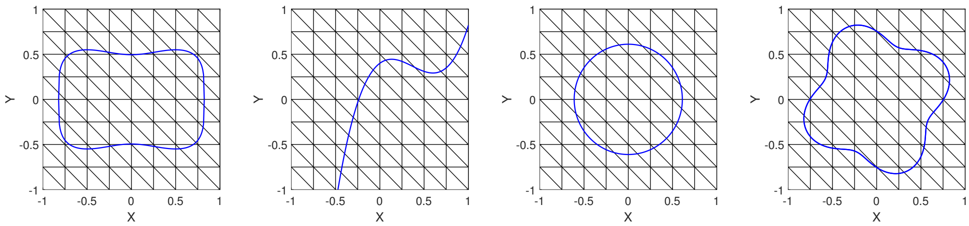

Figure 3: Uniform meshes for several shapes of interfaces of Example 5.1 through Example 5.4.

5. Numerical Results

In this section, we provide some numerical experiments for problems with the nonhomogeneous jumps. The experiment are conducted with various interface Γ and coefficients β. Figure 3 shows the interface shapes.

We name our new version of DB-IFEM as discontinuous bubble-modified immersed finite element method (DB-MIFEM). We report the L^2-error and piecewise H^1-errors of the DB-MIFEM (see Table 1, Table 3, Table 5, Table 7) and we compare them with those of the early DB-IFEM in [33] (see Table 2, Table 4, Table 6, Table 8).

We let the domain $\Omega = [-1,1]^2$ and we consider a uniform triangulation $\mathcal{T}_h$ by right triangles whose size $h = 2^{-k}, k = 3, 4, ..., 8$. We use the level set function $L(x,y) : \Omega \to \mathbb{R}$ and level set $\Gamma = \{(x,y) \,|\, L(x,y) = 0\}$ to represent the interface.

Example 5.1. *(Peanut shaped curve) The interface is given by* $\Gamma = \{(x,y) : x^4/2 - x^2/4 + y^2 - 0.06 = 0\}$ *and the coefficient is* $\beta^- = 1$, $\beta = 10^+$. *The exact solution is*

$$u(x,y) = \begin{cases} (4 - x^2 - y^2)/\beta^- & \text{if } (x,y) \in \Omega^-, \\ \\ 2\cos(x+y)/\beta^+ & \text{if } (x,y) \in \Omega^+. \end{cases}$$

We report the errors of DB-MIFEM in Table 1. We observe that the convergence rates are both optimal in L^2 and H^1-norms. On the other hand, Table 2 shows that results for the early DB-IFEM, where the convergence rates are suboptimal. Thus, the DB-MIFEM outperforms the early version.

Table 1: Example 5.1, DB-MIFEM

$1/h$	$\|\mathbf{u}-\mathbf{u}_h\|_{L_2(\Omega)}$	*order*	$\|\mathbf{u}-\mathbf{u}_h\|_{1,h}$	*order*
8	3.426×10^{-3}		9.276×10^{-2}	
16	8.743×10^{-4}	*1.970*	4.698×10^{-2}	*0.981*
32	2.150×10^{-4}	*2.024*	2.370×10^{-2}	*0.987*
64	5.434×10^{-5}	*1.984*	1.191×10^{-2}	*0.993*
128	1.347×10^{-5}	*2.013*	5.966×10^{-3}	*0.997*
256	3.448×10^{-6}	*1.966*	2.987×10^{-3}	*0.998*

Table 2: Example 5.1, DB-IFEM (early version)

$1/h$	$\|\mathbf{u}-\mathbf{u}_h\|_{L_2(\Omega)}$	*order*	$\|\mathbf{u}-\mathbf{u}_h\|_{1,h}$	*order*
8	5.684×10^{-3}		1.118×10^{-1}	
16	1.467×10^{-3}	*1.954*	5.436×10^{-2}	*1.040*
32	3.983×10^{-4}	*1.881*	3.262×10^{-2}	*0.736*
64	1.128×10^{-4}	*1.819*	1.895×10^{-2}	*0.784*
128	3.417×10^{-5}	*1.723*	1.138×10^{-2}	*0.736*
256	1.456×10^{-5}	*1.231*	7.691×10^{-3}	*0.565*

Example 5.2. *(cubic curve) The interface is given by* $\Gamma = \{(x,y) : y - 3x(x-0.3)(x-0.8) - 0.4 = 0\}$ *and the coefficient is* $\beta^- = 10$, $\beta^+ = 1$. *The exact solution is*

$$u(x,y) = \begin{cases} x^2 + y^2/\beta^- & \text{if } (x,y) \in \Omega^-, \\ 2\sin(x+y)/\beta^+ & \text{if } (x,y) \in \Omega^+. \end{cases}$$

We report the errors of DB-MIFEM in Table 3 and those for early DB-IFEM in Table 4. We observe that the convergence rates of DB-MIFEM are both optimal in L^2 *and* H^1*-norms. On the other hand, the early DB-IFEM has suboptimal convergent rates.*

Table 3: Example 5.2, DB-MIFEM

$1/h$	$\|\mathbf{u}-\mathbf{u}_h\|_{L_2(\Omega)}$	*order*	$\|\mathbf{u}-\mathbf{u}_h\|_{1,h}$	*order*
8	7.780×10^{-4}		5.512×10^{-2}	
16	1.644×10^{-4}	*2.243*	2.750×10^{-2}	*1.003*
32	3.624×10^{-5}	*2.182*	1.372×10^{-2}	*1.003*
64	8.407×10^{-6}	*2.108*	6.854×10^{-3}	*1.001*
128	2.038×10^{-6}	*2.045*	3.425×10^{-3}	*1.001*
256	5.004×10^{-7}	*2.026*	1.712×10^{-3}	*1.000*

Table 4: Example 5.2, DB-IFEM (early version)

$1/h$	$\|\mathbf{u}-\mathbf{u}_h\|_{L_2(\Omega)}$	*order*	$\|\mathbf{u}-\mathbf{u}_h\|_{1,h}$	*order*
8	2.177×10^{-3}		6.147×10^{-2}	
16	5.852×10^{-4}	*1.895*	3.436×10^{-2}	*0.839*
32	1.818×10^{-4}	*1.687*	1.967×10^{-2}	*0.805*
64	6.729×10^{-5}	*1.436*	1.226×10^{-2}	*0.682*
128	2.566×10^{-5}	*1.391*	7.788×10^{-3}	*0.654*
256	1.126×10^{-5}	*1.189*	5.284×10^{-3}	*0.560*

Example 5.3. *(Circle) The interface is given by* $\Gamma = \{(x,y) : x^2 + y^2 = 0.61111^2\}$ *and the coefficient is* $\beta^- = x^2 + y^2$, $\beta^+ = 1$. *The exact solution is*

$$u(x,y) = \begin{cases} 6x^2 + 7y^2 & \text{if } (x,y) \in \Omega^-, \\ \sin(3xy) + \cos(5x^2y^2) & \text{if } (x,y) \in \Omega^+. \end{cases}$$

We report errors of DB-MIFEM in Table 5 and those for early DB-IFEM in Table 6. We observe the similar behavior as before.

Table 5: Example 5.3, DB-MIFEM

$1/h$	$\|\mathbf{u}-\mathbf{u}_h\|_{L_2(\Omega)}$	*order*	$\|\mathbf{u}-\mathbf{u}_h\|_{1,h}$	*order*
8	1.023×10^{-1}		8.157×10^{-1}	
16	5.268×10^{-3}	*4.279*	2.750×10^{-1}	*1.129*
32	1.322×10^{-3}	*1.995*	1.372×10^{-1}	*0.993*
64	3.418×10^{-4}	*1.951*	6.854×10^{-2}	*0.998*
128	8.412×10^{-5}	*2.009*	3.425×10^{-2}	*0.999*
256	2.109×10^{-5}	*2.009*	1.712×10^{-2}	*0.999*

Table 6: Example 5.3, DB-IFEM (early version)

$1/h$	$\|\mathbf{u}-\mathbf{u}_h\|_{L_2(\Omega)}$	*order*	$\|\mathbf{u}-\mathbf{u}_h\|_{1,h}$	*order*
8	1.046×10^{-1}		8.490×10^{-1}	
16	8.008×10^{-3}	*3.708*	4.030×10^{-1}	*1.075*
32	2.025×10^{-3}	*1.983*	2.145×10^{-1}	*0.910*
64	5.200×10^{-4}	*1.961*	1.097×10^{-1}	*0.966*
128	1.663×10^{-4}	*1.645*	6.123×10^{-2}	*0.842*
256	7.581×10^{-5}	*1.133*	3.698×10^{-2}	*0.727*

Example 5.4. *(Star shaped curve) The interface is given by* $\Gamma = \{(r,\theta) : r - 0.57 - 0.1\sin(4\theta) = 0\}$ *and the coefficient is* $\beta^- = xy + 3$, $\beta^+ = x^2 - y^2 + 3$. *The exact solution is*

$$u(x,y) = \begin{cases} x^2 + y^2 + 2 & \text{if } (x,y) \in \Omega^-, \\ 1 - x^2 - y^2 & \text{if } (x,y) \in \Omega^+. \end{cases}$$

Table 7: Example 5.4, DB-MIFEM

$1/h$	$\|\mathbf{u}-\mathbf{u}_h\|_{L_2(\Omega)}$	*order*	$\|\mathbf{u}-\mathbf{u}_h\|_{1,h}$	*order*
8	4.513×10^{-2}		8.157×10^{-1}	
16	1.850×10^{-3}	*4.608*	2.750×10^{-1}	*1.129*
32	4.444×10^{-4}	*2.058*	1.372×10^{-1}	*0.993*
64	1.091×10^{-4}	*2.027*	6.854×10^{-2}	*0.998*
128	2.788×10^{-5}	*1.968*	3.425×10^{-2}	*0.999*
256	6.886×10^{-6}	*2.017*	1.712×10^{-2}	*0.999*

Table 8: Example 5.4, DB-IFEM (early version)

$1/h$	$\|\mathbf{u}-\mathbf{u}_h\|_{L_2(\Omega)}$	*order*	$\|\mathbf{u}-\mathbf{u}_h\|_{1,h}$	*order*
8	4.563×10^{-2}		2.100×10^{-1}	
16	2.572×10^{-3}	*4.149*	1.011×10^{-1}	*1.055*
32	6.454×10^{-4}	*1.994*	5.079×10^{-2}	*0.993*
64	1.621×10^{-4}	*1.993*	2.545×10^{-2}	*0.997*
128	4.065×10^{-5}	*1.996*	1.275×10^{-2}	*0.998*
256	1.017×10^{-5}	*1.999*	6.378×10^{-3}	*0.999*

We observe the similar behavior as before.

For all the examples, we see that the DB-MIFEM shows optimal convergence rates in L^2 and H^1-norms. However, for some examples, we see that the early DB-IFEM has suboptimal convergence rates. Thus, the modification of DB-IFEM via the enrichment of bilinear form enhances the accuracy for the problems with nonhomogeneous jumps. We show the graphs of numerical solutions of DB-MIFEM in Fig. 4. For all the examples, we see that the results does not have any oscillatory phenomena near the interfaces.

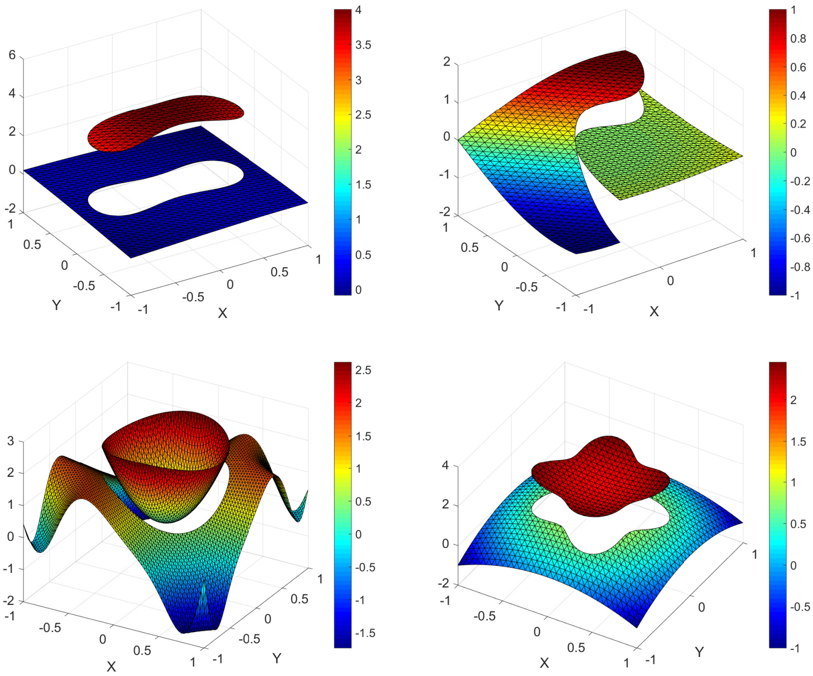

Figure 4: Numerical solutions for Example 5.1 (top, left), Example 5.2 (top, right), Example 5.3 (bottom, left) and Example 5.4 (bottom, right).

6. Conclusion

In this work, we studied a new version of DB-IFEM. We modified DB-IFEM in [33] by adding consistency terms to enhance the accuracy. We constructed a discontinuous bubble function which approximates the jump parts and by subtracting it from the bilinear form, we obtain a problem with homogeneous jump. We then proved the interpolation property of the DB function. We believe this is a first time to prove Bramble-Hilbert type of lemma for discontinuous functions. Then by showing the coerciveness of the new bilinear form we obtain the optimal error estimates for the new DB-IFEM.

The new DB-IFEM. clearly shows improvement in convergence rates over the early scheme for all the examples.

Acknowledgment

The second author is supported by the National Research Foundation of Korea(NRF) grant funded by the Korea government(MSIT) (NRF-2020R1C1C1A01005396)

References

[1] K. Garrett and H. Rosenberg, *The thermal conductivity of epoxy-resin/powder composite materials*, Journal of Physics D: Applied Physics, 7 (1974), p. 1247.

[2] T. Belytschko, N. Moës, S. Usui, and C. Parimi, *Arbitrary discontinuities in finite elements*, International Journal for Numerical Methods in Engineering, 50 (2001), pp. 993–1013.

[3] Z. Hashin, *Thin interphase/imperfect interface in elasticity with application to coated fiber composites*, Journal of the Mechanics and Physics of Solids, 50 (2002), pp. 2509–2537.

[4] A. Buffa, *Remarks on the discretization of some noncoercive operator with applications to heterogeneous maxwell equations*, SIAM Journal on Numerical Analysis, 43 (2005), pp. 1–18.

[5] Z. Chen, *Reservoir simulation: mathematical techniques in oil recovery*, SIAM, 2007.

[6] H. Duan and B. L. Karihaloo, *Effective thermal conductivities of heterogeneous media containing multiple imperfectly bonded inclusions*, Physical Review B, 75 (2007), p. 064206.

[7] F. Pavanello, F. Manca, P. Luca Palla, and S. Giordano, *Generalized interface models for transport phenomena: Unusual scale effects in composite nanomaterials*, Journal of Applied Physics, 112 (2012), p. 084306.

[8] R. Plonsey, *Bioelectric sources arising in excitable fibers (Alza lecture)*, Annals of biomedical engineering, 16 (1988), pp. 519–546.

[9] M. R. Hossan, R. Dillon, and P. Dutta, *Hybrid immersed interface-immersed boundary methods for ac dielectrophoresis*, Journal of Computational Physics, 270 (2014), pp. 640–659.

[10] G. Chavent and J. Jaffré, *Mathematical models and finite elements for reservoir simulation: single phase, multiphase and multicomponent flows through porous media*, Elsevier, 1986.

[11] C. Van Duijn, J. Molenaar, and M. De Neef, *The effect of capillary forces on immiscible two-phase flow in heterogeneous porous media*, Transport in Porous Media, 21 (1995), pp. 71–93.

[12] M. F. Wheeler, *An elliptic collocation-finite element method with interior penalties*, SIAM Journal on Numerical Analysis, 15 (1978), pp. 152–161.

[13] B. Cockburn, G. E. Karniadakis, and C.-W. Shu, *The development of discontinuous Galerkin methods*, in Discontinuous Galerkin Methods, Springer, 2000, pp. 3–50.

[14] D. N. Arnold, F. Brezzi, B. Cockburn, and L. D. Marini, *Unified analysis of discontinuous Galerkin methods for elliptic problems*, SIAM journal on numerical analysis, 39 (2002), pp. 1749–1779.

[15] A. Ern, I. Mozolevski, and L. Schuh, *Discontinuous Galerkin approximation of two-phase flows in heterogeneous porous media with discontinuous capillary pressures*, Computer methods in applied mechanics and engineering, 199 (2010), pp. 1491–1501.

[16] N. MOËS, J. DOLBOW, AND T. BELYTSCHKO, *A finite element method for crack growth without remeshing*, International journal for numerical methods in engineering, 46 (1999), pp. 131–150.

[17] T. BELYTSCHKO AND T. BLACK, *Elastic crack growth in finite elements with minimal remeshing*, International journal for numerical methods in engineering, 45 (1999), pp. 601–620.

[18] P. KRYSL AND T. BELYTSCHKO, *An efficient linear-precision partition of unity basis for unstructured meshless methods*, Communications in Numerical Methods in Engineering, 16 (2000), pp. 239–255.

[19] T. BELYTSCHKO, C. PARIMI, N. MOËS, N. SUKUMAR, AND S. USUI, *Structured extended finite element methods for solids defined by implicit surfaces*, International journal for numerical methods in engineering, 56 (2003), pp. 609–635.

[20] G. LEGRAIN, N. MOES, AND E. VERRON, *Stress analysis around crack tips in finite strain problems using the extended finite element method*, International Journal for Numerical Methods in Engineering, 63 (2005), pp. 290–314.

[21] Z. LI, T. LIN, AND X. WU, *New cartesian grid methods for interface problems using the finite element formulation*, Numerische Mathematik, 96 (2003), pp. 61–98.

[22] Z. LI, T. LIN, Y. LIN, AND R. C. ROGERS, *An immersed finite element space and its approximation capability*, Numerical Methods for Partial Differential Equations, 20 (2004), pp. 338–367.

[23] S. H. CHOU, D. Y. KWAK, AND K. T. WEE, *Optimal convergence analysis of an immersed interface finite element method*, Advances in Computational Mathematics, 33 (2010), pp. 149–168.

[24] D. Y. KWAK, K. T. WEE, AND K. S. CHANG, *An analysis of a broken P_1-nonconforming finite element method for interface problems*, SIAM Journal on Numerical Analysis, 48 (2010), pp. 2117–2134.

[25] D. Y. KWAK AND J. LEE, *A modified P_1-immersed finite element method*, International Journal of Pure and Applied Mathematics, 104 (2015), pp. 471–494.

[26] D. Y. KWAK, S. JIN, AND D. KYEONG, *A stabilized P_1-nonconforming immersed finite element method for the interface elasticity problems*, ESAIM: Mathematical Modelling and Numerical Analysis, 51 (2017), pp. 187–207.

[27] D. KYEONG AND D. Y. KWAK, *An immersed finite element method for the elasticity problems with displacement jump*, Advances in Applied Mathematics and Mechanics, 9 (2017), pp. 407–428.

[28] S. JIN, D. Y. KWAK, AND D. KYEONG, *A consistent immersed finite element method for the interface elasticity problems*, Advances in Mathematical Physics, 2016 (2016).

[29] G. JO AND D. Y. KWAK, *An IMPES scheme for a two-phase flow in heterogeneous porous media using a structured grid*, Computer Methods in Applied Mechanics and Engineering, (2017).

[30] D. Y. KWAK, S. LEE, AND H. YUNKYONG, *A new finite element for interface problems having robin type jump*, Inernational Journal of Numerical Analysis and Modeling, 14 (2017), pp. 532–549.

[31] M. CROUZEIX AND P. A. RAVIART, *Conforming and nonconforming finite element methods for solving the stationary Stokes equations I*, Revue française d'automatique, informatique, recherche opérationnelle. Mathématique, 7 (1973), pp. 33–75.

[32] S. H. CHOU, D. Y. KWAK, AND K. Y. KIM, *Mixed finite volume methods on nonstaggered quadrilateral grids for elliptic problems*, Mathematics of computation, 72 (2003), pp. 525–539.

[33] K. S. CHANG AND D. Y. KWAK, *Discontinuous bubble scheme for elliptic problems with jumps in the solution*, Computer Methods in Applied Mechanics and Engineering, 200 (2011), pp. 494–508.

[34] T. LIN, Q. YANG, AND X. ZHANG, *A priori error estimates for some discontinuous Galerkin immersed finite element methods*, Journal of Scientific Computing, 65 (2015), pp. 875–894.

[35] T. LIN, Y. LIN, AND X. ZHANG, *Partially penalized immersed finite element methods for elliptic interface problems*, SIAM Journal on Numerical Analysis, 53 (2015), pp. 1121–1144.

[36] J. A. ROITBERG ET AL., *A theorem on homeomorphisms for elliptic systems and its applications*, Mathematics of the USSR-Sbornik, 7 (1969), p. 439.

[37] J. H. BRAMBLE AND J. T. KING, *A finite element method for interface problems in domains with smooth boundaries and interfaces*, Advances in Computational Mathematics, 6 (1996), pp. 109–138.